



HAL
open science

Magnetic Slow Relaxation in a Metal-Organic Framework Made of Chains of Ferromagnetically Coupled Single-Molecule Magnets

Gang Huang, Guglielmo Fernandez-Garcia, Insa Badiane, Magatte Camarra, Stéphane Freslon, Olivier Guillou, Carole Daiguebonne, Federico Totti, Olivier Cador, Thierry Guizouarn, et al.

► **To cite this version:**

Gang Huang, Guglielmo Fernandez-Garcia, Insa Badiane, Magatte Camarra, Stéphane Freslon, et al.. Magnetic Slow Relaxation in a Metal-Organic Framework Made of Chains of Ferromagnetically Coupled Single-Molecule Magnets. *Chemistry - A European Journal*, 2018, 24 (27), pp.6983-6991. 10.1002/chem.201800095 . hal-01807090

HAL Id: hal-01807090

<https://univ-rennes.hal.science/hal-01807090v1>

Submitted on 19 Jun 2018

HAL is a multi-disciplinary open access archive for the deposit and dissemination of scientific research documents, whether they are published or not. The documents may come from teaching and research institutions in France or abroad, or from public or private research centers.

L'archive ouverte pluridisciplinaire **HAL**, est destinée au dépôt et à la diffusion de documents scientifiques de niveau recherche, publiés ou non, émanant des établissements d'enseignement et de recherche français ou étrangers, des laboratoires publics ou privés.

Magnetic slow relaxation in a Metal Organic Framework made of chains of ferromagnetically coupled Single-Molecule Magnets

Gang Huang,^a Guglielmo Fernandez-Garcia,^{b,c} Insa Badiane,^{a,d} Magatte Camarra,^{a,d} Stéphane Freslon,^a Olivier Guillou,^a Carole Daignebonne,^a Federico Totti,^c Olivier Cador,^b Thierry Guizouarn,^b Boris Le Guennic^{*b} and Kevin Bernot^{*a}

Abstract: We report the study of a Dy-based metal-organic framework (MOF), with unprecedented magnetic properties. The compound is made of nine-coordinated Dy^{III} magnetic building blocks (MBBs) with poor intrinsic single-molecule magnet behaviour. However, the MOF architecture constrains the MBBs in a one-dimensional structure that induces a ferromagnetic coupling between them. Overall, the material shows a magnetic slow relaxation in absence of external static field and a hysteretic behaviour at 0.5K. Low temperature magnetic studies, diamagnetic doping and ab-initio calculations highlight the crucial role played by the Dy-Dy ferromagnetic interaction. Overall, we report an original magnetic object at the frontier between single-chain magnet and single-molecule magnet that host intra-chain couplings that cancel quantum tunneling between the MBBs. This compound evidences that bottom-up approach via MOF design can induce spontaneous organization of MBBs able to produce remarkable molecular magnetic material.

Introduction

The organization of molecular magnetic building blocks (MBBs) into extended framework to form Metal-Organic Framework (MOF) is a dynamic field of research.^{1,2} MOFs have been proposed as a potential way to constrain coordination geometries of metallic ions to form arrays of single-molecule magnets (SMMs)³⁻⁵ or single-chain magnets (SCMs)^{6,7}. This approach is particularly relevant when MBBs are made of lanthanide ions.^{8,9}

In fact, high performance lanthanide-SMMs possess highly symmetric electrostatic environments that induce strong stabilization of the magnetic ground state.¹⁰⁻¹³ A striking

illustration of the latter concept is given by the Ln-phtalocyanine (LnPc) systems¹⁴⁻¹⁷ where the organic ligands impose a strict D_{4d} site symmetry to the lanthanide ion and dramatically improve its magnetic properties when compared to distorted coordination environment.¹⁸ Compounds based on cyclooctatetraene (COT) are also remarkable examples of such approach with D_{8d} symmetry able to induce strong SMM behaviour on a wide range of lanthanide ions such as Ce^{III},¹⁹ Nd^{III},²⁰ Dy^{III},²¹ and Er^{III}.²² The library of such systems is continuously growing^{9,23-27} with the recently added pentagonal bipyramidal environment (D_{5h}) that provides excellent SMM behaviour on Dy^{III} adducts.²⁸ Last, an astonishing example of electrostatic engineering around a Dy^{III} centre has been reported with observation of magnetic slow relaxation at record temperatures.²⁹

However, as far as applications are targeted, a given Ln-SMM has to be converted into a material and then a device. To do so, different pathways can be followed. The first one is to isolate or organize the SMM on surfaces, a strategy that supposes solubility,^{30,31} evaporability^{32,33} or substitution by grafting groups.^{34,35} However, this does not guarantee that the SMM properties are kept on surfaces³⁶ as observed on the previously cited LnPc where excellent,^{37,38} erratic³⁹ or depth-dependent magnetic behaviour on films is observed.⁴⁰ Robustness of magnetic behaviour of Ln-SMM upon surface deposition is thus rarely observed.^{41,42}

The second way is to organize the MBBs in the crystal packing^{43,44} in order to optimize the overall magnetic behaviour of the compound. Ideally, this may give rise to compounds where the MBBs are organized such as molecular magnetic anisotropy axes point in the same direction in order to avoid cancellation of the magnetic moments. Little real control is observed on that point. Indeed, real step-by-step procedure that relies on the isolation of a Ln-MBB and its organization into a MOF is rather scarce⁴³ as reviewed recently.⁵ In most cases, magnetic MOFs are made of mono-⁴⁵⁻⁵⁰ or polynuclear^{39,2,51-57} MBBs that spontaneously organize in the crystal packing.

Magnetic MOFs have two main assets: their structural rigidity and their original topology. i) The structural rigidity around the metallic centre has been recently identified as a key factor for the observation of magnetic slow relaxation because it minimizes the phonon coupling responsible for the promotion of under-barrier relaxation pathways.⁵⁸ ii) The topology of the magnetic MOFs is able to induce magnetic behaviour unobservable on the isolated MBBs such as dynamic magnetic behaviour upon external stimuli⁵⁹ or upon host-guest removal.⁶⁰ Even non-porous MOFs can be appealing as the constrain on the chemical environment¹ of the MBB can induce strong magnetocaloric effect (MCE)⁶¹⁻⁶⁴ or three-dimensional (3D) magnetic ordering.^{49,65-71} This last feature implies strong magnetic interactions between the MBBs and we will focus on

[a] Dr G.Huang, Dr. I. Badiane, S Freslon, Pr. O. Guillou, Dr. C. Daignebonne, Dr. K.Bernot

Univ Rennes, INSA Rennes, CNRS, ISCR (Institut des Sciences Chimiques de Rennes) UMR 6226, F-35000 Rennes, France
E-mail: kevin.bernot@insa-rennes.fr

[b] Dr G.Fernandez-Garcia, Pr. O. Cador, T. Guizouarn, Dr. B. Le Guennic

Univ Rennes, CNRS, ISCR (Institut des Sciences Chimiques de Rennes) UMR 6226, F-35000 Rennes, France

[c] Dr G.Fernandez-Garcia, Pr. F. Totti, Laboratory of Molecular Magnetism (LaMM), Università degli studi di Firenze, INSTM unit, Via della lastruccia 3, 50019 Sesto Fiorentino, Italy.

[d] Dr. I. Badiane, Dr. M. Camarra, LCPM – Groupe "Matériaux Inorganiques: Chimie Douce et Cristallographie" Université Assane Seck de Ziguinchor, BP 523 Ziguinchor, Sénégal.

Supporting information for this article is given via a link at the end of the document.

this particular point in this paper.

We report herein a MOF where spontaneous organization of the Dy-MBBs into chains is observed. This peculiar feature induces ferromagnetic intra-chain interaction that promotes a fast relaxing MBB into a material with magnetic slow relaxation and opening of a hysteresis at low temperature.

Results and Discussion

Structural description

The reaction of 1,2-phenylenediacetic acid ($\text{H}_2\text{O-PDA}$) with lanthanide chloride salts affords an isostructural series of three dimensional MOF of general formula $[[\text{Ln}(\text{o-PDA})_3(\text{H}_2\text{O})_2] \cdot 2\text{H}_2\text{O}]_n$. The crystal structures have been reported for $\text{Ln}=\text{La}^{\text{III}}$,⁷² Nd^{III} ,⁷² Dy^{III} ,⁷³ Pr^{III} ,⁷⁴ Er^{III} ,⁷⁴ Tb^{III} ,⁷⁵ Ho^{III} ,⁷⁵ with all derivatives obtained through hydrothermal synthesis. In this work, we have been able to obtain the same isostructural microcrystalline powders using soft chemistry reaction (see SI) for $\text{Ln}=\text{Dy}^{\text{III}}$ (latter called **Dy**) (Figure S1) and for a doped derivative $[[\text{Dy}_{0.08}\text{Y}_{0.92}(\text{o-PDA})_3(\text{H}_2\text{O})_2] \cdot 2\text{H}_2\text{O}]_n$ latter called **Y:Dy** (Figure S2). Hereafter, we provide a brief description of the crystal structure.⁷³

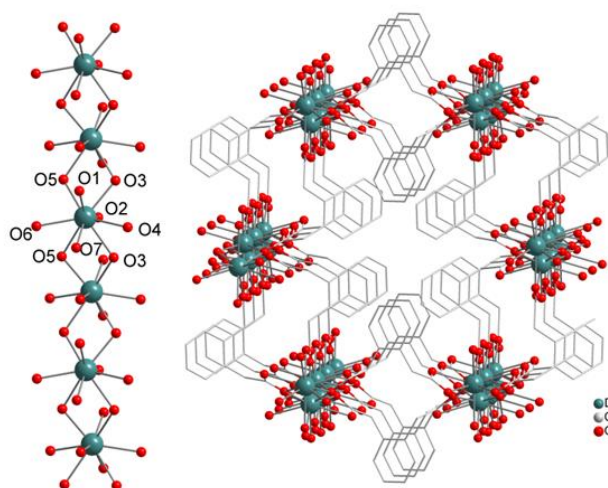


Figure 1. (left) Representation of the Dy^{III} chain that spreads along c axis with labelling scheme. (right) Perspective crystal packing view close to the c axis. Hydrogen atoms omitted for clarity.

Dy crystallizes in the monoclinic C2/c space group. The asymmetric unit is made of one and a half o-PDA^{2-} ligand, one coordinated water molecule, half Dy^{III} ion and one uncoordinated water molecule. Each Dy^{III} ion is surrounded by nine oxygen atoms: one from a coordinated water molecule (O7) and eight from six different o-PDA^{2-} ligands. Four oxygen atoms (O1, O2, O4, O6) bind only one Dy^{III} ion (μ_1 mode) and four oxygen atoms (O3, O3a, O5, O5a) bind two Dy^{III} ions (μ_2 mode) (Figure 1 and Table S1). From the magnetic point of view, this last coordination mode is expected to transmit sizeable magnetic

interaction between the Dy^{III} ions.⁷⁶⁻⁷⁸ The Dy^{III} ion presents a muffin-like coordination polyhedron (C_s)⁷⁹ (Figure 3, Table S2). Overall, Dy^{III} chains spread along the c axis (Figure 1) and each o-PDA^{2-} ligand connects two parallel chains. The shortest Dy-Dy distance within a chain is 4.01(1) Å and the inter-chain Dy-Dy distances are 7.82(2), 9.42(3) and 9.96(3) Å depending of the considered neighbouring chain (Ch1, Ch2 and Ch3, see Figure 4). The network can be described as a (6, 3) topologic structure with a honeycomb-like core (Figure 1).

Static magnetic properties

Room temperature $\chi_{\text{M}}T$ value measured on **Dy** is $13.64 \text{ cm}^3 \cdot \text{K} \cdot \text{mol}^{-1}$ close to the one of the free-ion ($14.17 \text{ cm}^3 \cdot \text{K} \cdot \text{mol}^{-1}$). Upon cooling, a decrease of $\chi_{\text{M}}T$ is observed in line with the thermal depopulation of the M_J states (Figure 2). Below 20K, an abrupt increase is observed and $\chi_{\text{M}}T$ reaches $30.6 \text{ cm}^3 \cdot \text{K} \cdot \text{mol}^{-1}$ at 2.0 K and a maximum of $50.69 \text{ cm}^3 \cdot \text{K} \cdot \text{mol}^{-1}$ at 1.0 K. This sharp rise of $\chi_{\text{M}}T$ is followed by a drop until $40.37 \text{ cm}^3 \cdot \text{K} \cdot \text{mol}^{-1}$ at 0.63 K. It is worth noting that $\chi_{\text{M}}T$ reconstruction from zero-field dynamic magnetic measurement affords very similar temperature dependence (Figure S3) and discards the occurrence of saturation effects. Consequently both ferro- and antiferromagnetic couplings operate in **Dy**. The doped derivative, **Y:Dy**, depicts a monotonous decrease of $\chi_{\text{M}}T$ that reaches a plateau below 11K, and validates its use as a magnetically uncoupled analogue of **Dy** (Figure 2).

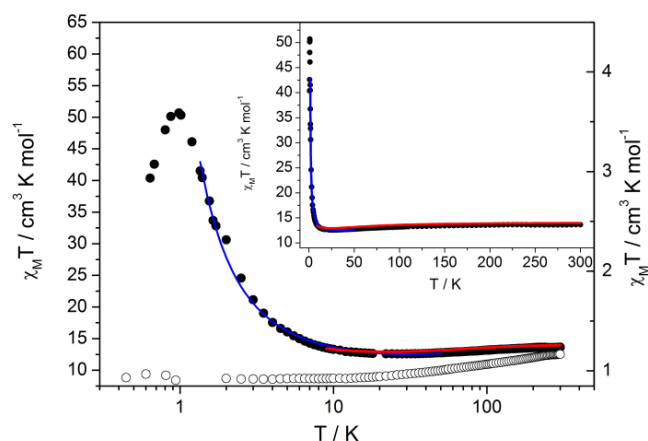


Figure 2. Temperature dependence of $\chi_{\text{M}}T$ measured via static magnetic measurements for **Dy** (full symbol, left axis) and **Y:Dy** (empty symbol, right axis). Note the logarithmic temperature scale. *ab-initio* calculations are represented as a red line and best fit with Ising model as a blue line (see text).

ab-initio calculations and electrostatics

In first approximation, the strong ferromagnetic coupling observed on **Dy** is expected to be a consequence of the μ_2 bridging mode of the oxygen atoms (O3 and O5) that bind the Dy^{III} .^{66,67,80}

To shed some light on this point, *ab-initio* SA-CASSCF/SI-SO calculations have been performed (see SI for details). A Dy^{III} ion has been considered together with its two closest neighbours within the chain as Y^{III} ions (Figure 3). All coordinated oxygen

atoms have been considered explicitly. In fact, some of us have previously demonstrated that a too simplified description of the neighbouring environment of a given Dy^{III} in a Dy-chain can lead to a wrong description of the electrostatic features of the compound.⁸¹ This system can be then considered as a good model of the doped compound **Y:Dy**.

The Dy^{III} ion is found extremely anisotropic ($g_x=0$, $g_y=0.01$, $g_z=19.66$) with an almost pure 15/2 ground state that is very well separated from the first excited one by 203 K (141 cm⁻¹) (Table S3 and Figure S5). This is a rare feature for a nine-coordinated Dy^{III} ion.⁸² The chain direction can be considered as the line connecting the i^{th} and $(i+2)^{\text{th}}$ Dy^{III}. The angle of the calculated easy-magnetic axis between two consecutive Dy^{III} is 16.89° so that the angle with the chain direction is 34.12° (Figure 4). This slightly canted orientation is in line with a dipolar ferromagnetic Dy-Dy interaction along the chain.

It is well-known that the Ln-O binding is mainly electrostatic in nature and that the main anisotropy direction is governed by the minima in the electrostatic potential field. We employed then the home-developed CAMMEL code (CALculated Molecular Multipolar ELEctrostatics, see SI) to analyse, at the radius of 1.6 Å from the ligands, the electrostatics extracted from the *ab-initio* calculations.

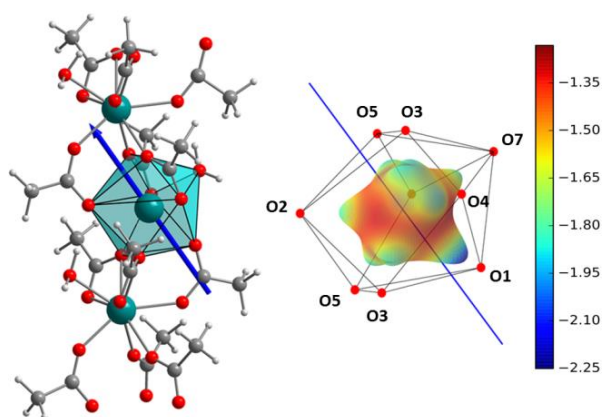


Figure 3. (left) Representation of the calculated easy-magnetic axis on a Y-Dy^{III}-Y moiety. (right) Representation of the total electrostatics potential at 1.6 Å around the Dy^{III} ion (the lowest and highest values are in blue and red, respectively), with the easy-axis direction as blue line.

It is clear from Figure 3 that the orientation of the *g* tensor is heavily influenced by the contribution of a single oxygen atom (O1); the latter is indeed at the shortest distance of the Dy^{III} ion (Table S1) and generates a more negative potential. However, looking at the single contributions in the multipolar expansion (Figure S4), it is clear that this effect is not driven by the different charges distribution on the oxygen atoms, but by the quadrupole moment (and in a lesser extent by the dipoles).

Magnetic interactions in **Dy** are attributable mainly to dipolar coupling because of the large distances between metal sites.

These interactions have been calculated taking a Dy^{III} ion as reference and considering all its neighbours in a radius of 15 Å, using the Lines model (see SI). The interactions along the chain are all found ferromagnetic, with the one with the first neighbour's particularly strong ($J_{1,\text{dip}}=3.665$ cm⁻¹ in the effective $S=1/2$ framework, see also Figure 4, Table S4 and Figure S6). The latter is also the only interaction that is expected to be not only dipolar in nature due to a short distance of 4 Å. The interactions with the neighbouring chains called Ch1, Ch2 and Ch3 are found both ferro- and antiferromagnetic, but with a prevalence of antiferromagnetism. Indeed, the sum of all interactions from neighbouring chains interaction leads to inter-chain coupling of $J_{\text{inter}}=-0.048$ cm⁻¹.

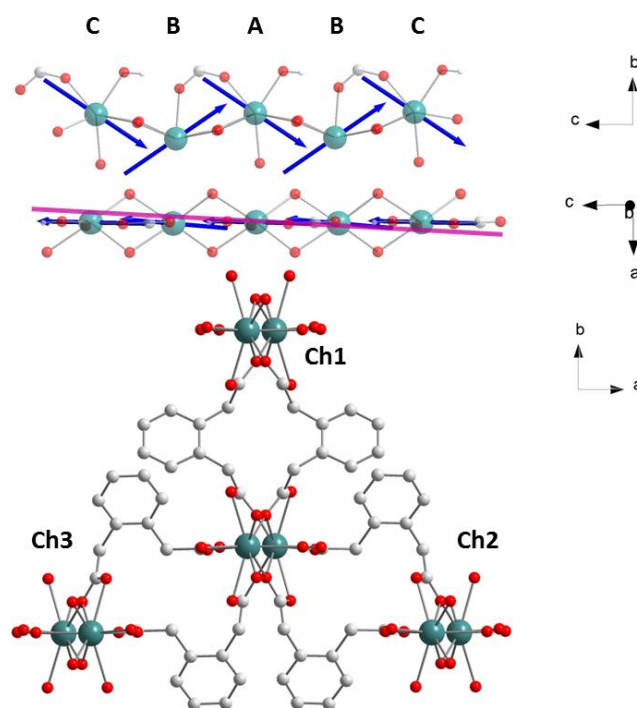


Figure 4. (top) Representation of the calculated easy-magnetic axes (blue). (middle) Representation of the easy-magnetic axes (blue) and of the resulting magnetic component along the chain. (bottom) Representation of the different chains considered for the calculations of dipolar coupling in **Dy**.

SMM vs SCM behaviour

At that stage, given the strong intramolecular ferromagnetic interaction observed on **Dy**, and the relatively high distances observed between the chains, one may expect single-chain magnet (SCM) behaviour.⁸³⁻⁸⁶ Such behaviour is seen when magnetic slow relaxation of a chain-based compound is confined inside the chain. The compound consequently behaves as a one-dimensional molecular magnet that adopts an Ising-spin chain dynamics^{7,87-91} and can be described by the following spin Hamiltonian:

$$H_{\text{Ising}} = - \sum_{ij} J_{\text{Ising}(ij)} S_{iz} S_{jz} \quad (\text{eq.1})$$

where S_{iz} are the projection of the pseudospin eigenfunction on the axis of anisotropy of the i^{th} site, collinear with the j^{th} site. On a static magnetic point of view, this implies the creation of magnetic domains within a chain where a given number of spin carriers can relax collectively. These coherent domains create a "correlation length" ξ that is observed when the magnetic interaction along the chain is strong enough when compared to the temperature and possible weak inter-chain interactions.^{89,92,93} The growth of ξ induces an exponential variation of $\chi_M T$ according to:

$$\chi_M T \propto \exp(J_{\text{Ising}}/2k_B T) \quad (\text{eq.2})^{7,66,67,80,94,95}$$

On **Dy**, a J_{Ising} value of 2.89 cm^{-1} is found in the 2-10 K temperature range. Consequently, we can discard a SCM behaviour on **Dy** because J is considerably smaller than the energy barrier for spin reversal (*vide infra*) and the corresponding correlation length can be considered smaller than one repetitive unit

Within the Lines model we calculated the same interaction with $J_{\text{Ising}} = J_{\text{Lines}} \cos(\varphi)$ where φ is the angle that projects the non-collinear Lines framework in the collinear Ising model.⁹⁸ The fitted $J_{\text{Lines}} \approx 3.93 \text{ cm}^{-1}$ with $\varphi \approx 50^\circ$ (see Figure S8) provides $J_{\text{Ising}} = 2.53 \text{ cm}^{-1}$. The difference between J_{Lines} and J_1^{dip} (3.66 cm^{-1}) comes from the exchange interaction that cannot be calculated due to the complex network of dipolar couplings.

Overall, the observed magnetic behaviour at low temperature (0-1 K) is explained by considering the system as Ising ferromagnetic chains, coupled by antiferromagnetic weak interactions.

Dynamic magnetic properties

Dynamic magnetic measurements have been performed on **Dy** and **Y:Dy**. In zero field ($H_{\text{dc}}=0 \text{ Oe}$), the two derivatives behave very differently. The relaxation time, τ , measured on **Dy** is not affected by any temperature independent phenomenon on all the investigated temperature range (0.67-5 K) (Figures S9-S12). This is an extremely rare feature as a levelling of τ is almost always observed on Dy^{III} -based SMMs.⁹ Such levelling has been evidenced to be due to the occurrence of quantum tunnelling, Raman or direct relaxation processes that overcome the Orbach one at low temperature.⁹⁹ For **Dy** the strong magnetic coupling that operates between the Dy^{III} ions favours a pure thermally dependant relaxation process that is expected to vary as $\tau = \tau_0 \exp(\Delta/k_B T)$ with τ_0 the characteristic relaxation time and Δ the energy barrier for spin reversal. For **Dy**, these parameters are estimated to be $\tau_0 = 1.6 \cdot 10^{-5} \text{ s}$ and $\Delta = 9.1 \text{ K}$ (6.3 cm^{-1}) (see Table S6). One can notice here that the physical meaning of Δ is far from an obvious point as we are looking to an ensemble of coupled SMMs and not to an isolated magnetic molecule. Additionally, the distribution of the relaxation times is small above 1.8 K as demonstrated by the Cole-Cole plots ($\alpha_{1.8\text{K}} = 0.27$, see Figure S14 and Table S7) but increases as AF couplings became relevant ($\approx 1 \text{ K}$). These Cole-Cole plots allow estimating for each temperature the isothermal (χ_T) and adiabatic susceptibility (χ_S) and consequently provide the relaxing fraction of the sample ($1 - (\chi_S/\chi_T)$). Almost all the sample relaxes slowly with a relaxing fraction of 99% and 93 % at 0.8 K and 1.8 K respectively (Table S7).

In-field measurements have been performed for $H_{\text{dc}}=1200 \text{ Oe}$, the field at which the slowest relaxation is observable at 2 K (Figure S15). This induces a crossing between the Arrhenius plots extracted for $H_{\text{dc}}=0 \text{ Oe}$ and $H_{\text{dc}}=1200 \text{ Oe}$ (Figure 5) at $T \approx 1 \text{ K}$. This is a rare feature as magnetic relaxation below 1 K is slower in zero-field than in-field and induce an opening of an hysteresis that is not narrowed in zero field (butterfly-like hysteresis) as commonly observed on Dy^{III} adducts.^{9,100,101}

In-field measurements show a thermally activated behaviour far superior to the one in zero field with $\tau_0 = 8.0 \cdot 10^{-8} \text{ s}$ and $\Delta = 49.6 \text{ K}$ (34.5 cm^{-1}) (Tables S8-S9). Despite a large relaxing fraction (84% and 96% at 0.8 K and 1.8 K respectively), a very high distribution of the relaxation times is observed ($\alpha = 0.60$ and 0.50 at 0.8 K and 1.8 K respectively) (Tables S8-S9, Figure S16-S20). This maybe a consequence of the competition between several relaxation processes.¹⁰²⁻¹⁰⁴ Indeed, a progressive levelling of τ is observed as the temperature is lowered (Figure 5). This is strikingly different from what observed commonly on Dy^{III} -SMMs where the application of a dc field induces a purest magnetic slow relaxation than in zero field.⁹⁹

Magnetic dilution is a useful approach to investigate the magnetic property of a given SMM without the influence of its magnetic neighbours.¹⁰⁵⁻¹¹⁷ Once crystallized in an isomorphous diamagnetic matrix, the SMM behaviour is generally optimized as intermolecular interactions that are likely to create additional and damaging pathways for the magnetic relaxation are suppressed.^{108,117} In the particular case of **Dy** the magnetic dilution is a simple way to: i) characterize the SMM properties of the isolated MBB ii) test the influence of the magnetic interactions (either along or between the chains) on the relaxing properties of the isolated Dy^{III} ion.

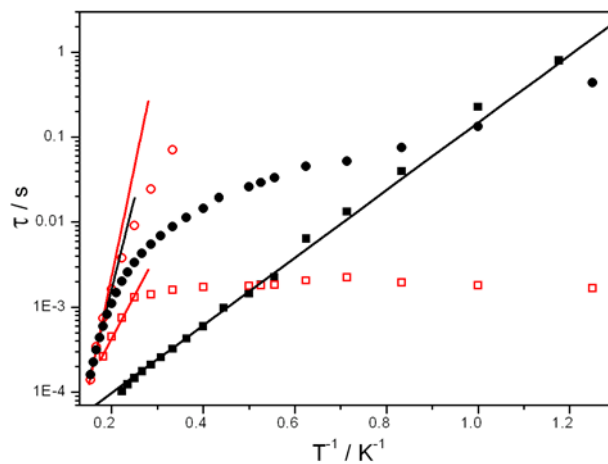


Figure 5. Plot of the relaxation times versus temperature for **Dy** (black symbols) and **Y:Dy** (red symbols) measured with $H_{\text{dc}}=0 \text{ Oe}$ (squares) and $H_{\text{dc}}=1200 \text{ Oe}$ (circles). Parameters for best fits are described in the text.

In zero field, the doped compound **Y:Dy** presents a thermal dependence of τ only above 4 K with Orbach parameters of $\tau_0 = 4.0 \cdot 10^{-6} \text{ s}$ and $\Delta = 23.4 \text{ K}$ (16.2 cm^{-1}) (Figures S21-S25, Tables

S10-S11). It is important to notice here that Δ is by far superior to the one observed on **Dy** indicating that the isolated ion possess a well isolated ground state and possible good SMM performance. However, quantum tunnelling relaxation processes are very efficient below 4 K and impose a totally thermally independent relaxation ($\tau \approx 100$ Hz). The relaxing fraction is very large (90% and 95% at 0.8 K and 1.8 K respectively) with a severely damaged relaxation time distribution when compared with **Dy** ($\alpha_{1.8, \kappa} = 0.58$ whereas it was 0.27 for **Dy**). In-field measurement on **Y:Dy**, present a typical enhancement of the magnetic relaxation at high temperature confirming the influence of quantum tunnelling in zero field with $\tau_0 = 1.6 \cdot 10^{-8}$ s and $\Delta = 59.5$ K (41.4 cm^{-1}) (Figure S26-S31, Tables S12-S13). These behaviours are in qualitative agreement with the *ab initio* magnetization barrier (Figure S5) that suggests a relaxation pathway involving either an Orbach process from the first excited state or a quantum tunnelling process from the second excited state. The fast thermally independent zero-field relaxation is not accounted by the *ab-initio* calculations. This may suggest that additional fast relaxation processes are involved such as the contribution from hyperfine coupling with yttrium nuclear spin.

These findings clearly demonstrate that ferromagnetic couplings in **Dy** enhance its magnetic relaxation. Overall, **Y:Dy** has a slowest magnetic relaxation than **Dy** at high temperature. However below 1K, when the couplings are relevant, **Dy** is a better SMM than **Y:Dy** whatever H_{dc} is. This is further confirmed by hysteresis measurements.

Hysteresis measurements

Hysteresis curves have been recorded for **Dy** and **Y:Dy** at 0.47 K with a field sweep rate of $16 \text{ Oe}\cdot\text{s}^{-1}$ (Figure 6). **Dy** shows an opened hysteresis between ± 5000 Oe with a coercitive field of 250 Oe, a remanant magnetization of $1.2 \mu_B$ and saturation at $4 \mu_B$. The hysteresis is no more visible at higher fields but a stepped magnetization curve is observed (6500 Oe) that further led to the expected $5 \mu_B$ saturation at 50000 Oe (Figure S32). This is a signature of AF couplings between the chains.

The hysteresis observed at low fields is then suspected to be due to the ferromagnetic coupling between the MBBs along the chain. This is further confirmed by the closed hysteresis over the whole investigated field region on **Y:Dy**.

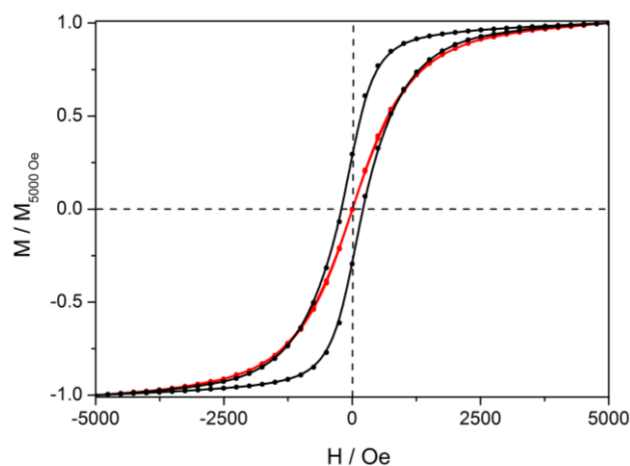


Figure 6. Hysteresis measurements of **Dy** and **Y:Dy** at 0.47 K with magnetic field sweep rate of $16 \text{ Oe}\cdot\text{s}^{-1}$

Dy can be described as a “pure 4f” analogue of 2d-3d,¹¹⁸ 3d-3d,¹¹⁹⁻¹²¹ 3d-5d,¹²² or 4f-5d¹²³ hetero-metallic chains. The strong anisotropy of the Dy-MBBs and the magnetic couplings in **Dy** preclude the occurrence of AF order as observed on some SCMs.^{119,124,125} Ferromagnetic couplings between the MBBs suppress the thermally independent relaxation pathways. Such behaviour has been observed in the past on, among others, antiferromagnetic interacting Mn_4 complexes,^{126,127} ferromagnetic coupled Fe_4 supramolecular chains,¹²⁸ cyanide-based SMM,¹²⁹ Dy-radical tetramers,¹³⁰ Dy^{III} dimers¹³¹ but, to the best of our knowledge, never on 4f-chains.

Conclusions

Dy is a rare example of a compound made of nine-coordinated Dy^{III} ions that presents magnetic slow relaxation. Comparative studies of **Dy** and its doped derivative **Y:Dy** shows that the Dy-MBB is strongly anisotropic, but relaxes quickly in zero-field via temperature-independent relaxation processes. Ferromagnetic coupling between the MBBs cancels these processes and a ferromagnetic chain of MBBs is created at low temperature where MBBs displays magnetic slow relaxation. The intra-chain coupling is mainly dipolar but *ab-initio* calculations evidence a small exchange contribution between nearest neighbours. Additionally, a close analysis of the inter-chain interactions highlights a global antiferromagnetic coupling between neighbouring chains at very low temperature. Contrary to **Y:Dy**, an hysteretic behaviour is observed on **Dy**, with opening in zero-field. Overall **Dy** is an original magnetic object at the frontier between single-chain magnet and single-molecule magnet. Indeed, it combines strong intra-chain couplings with efficient cancelling of magnetic quantum tunnelling. This is a key point as most of Dy^{III} -based slow relaxing compounds show zero-field closed (butterfly-like) hysteresis; that is a severe limitation for their use in low temperature magnetic memory devices.

Ferromagnetic interactions between Dy-SMM is then an efficient way to open their hysteresis in zero-field. In this study such interactions are tailored by the organization of the Dy ions in a Metal Organic Framework skeleton.

The MOF approach is also an efficient way to constrain catalytic clusters,¹³² chiral molecules¹³³ or MBBs^{1,2} into peculiar environments and consequently to induce original magnetic couplings. Usually, high-porosity MOF are targeted because of their versatile magnetic dynamics upon guest exchange^{60,134-136} or capability to host SMMs.¹³⁷⁻¹³⁹ However, we show here that low-porosity MOFs made of 4f-MBBs,¹⁴⁰ as Dy, should also be carefully considered. Last, the rigidity of these molecular edifices is an asset to minimize spin-phonon fast-relaxation mechanisms⁵⁸ and thus may give rise to high-performance molecular magnets.

Experimental Section

Synthetic procedure: All reagents have been purchased from TCI Chemicals and used without further purification. 1.5 mmol of 1,2-phenylenediacetic acid is deprotonated by equivalent NaOH in 20 ml H₂O. This solution is added directly into a stirred LnCl₃·6H₂O (1.5 mmol) aqueous solution to produce white precipitates. The precipitates are filtered and washed by distilled water and finally dried in the air. Yttrium doped derivative is obtained with similar procedure by using the appropriate lanthanide chloride salts in a 9:1 (Y:Dy) ratio.

X-ray powder diffraction: Experimental diffractograms have been collected with a Panalytical X'pert Pro diffractometer equipped with an X'Celerator detector and a copper source CuK α =1.542 Å. Recording conditions in θ - θ mode are 45kV, 40mA, step size 0.0084°, scan per step 50s. Calculated diffractograms have been produced using mercury software from CCDC.

EDS analysis: measurements have been carried out with a Hitachi TM-1000, Tabletop microscope version 02.11 (Hitachi High-Technologies, Corporation Tokyo Japan) with an EDS analysis system (SwiftED-TM, Oxford Instruments Link INCA). The instrument is equipped with a silicon drift detector with an energy resolution of 165 eV. Samples were observed by means of an electron beam accelerated at 15 kV, under high vacuum. Samples were put on carbon discs, stuck on an aluminum stub fixed at 7 mm from the beam, with an angle of measurement of 22°. Reproducibility of the elemental analyses was carefully checked by reproducing several times the measurements on 6 different sample location (see supplementary information).

Magnetic measurements: Magnetic measurements have been performed on a Quantum Design MPMS magnetometer using polycrystalline samples compacted in pellets to avoid crystallite orientation under magnetic field. Measurements have been corrected from the diamagnetic contributions calculated with Pascal constants. Hysteresis curves were measured with a ³He insert in the same magnetometer with a field sweep rate of 16 Oe.s⁻¹.

Electrostatics analysis with CAMMEL code: The home-made CALculated Molecular Multipolar Electrostatics code (CAMMEL) allows calculating the electrostatic potential generated by the ligands at a given radius from the metallic center, following the equation:

$$V(r_i) = \sum_i^N \frac{q_i}{|r_i - r|} + \frac{p_i \cdot r_i}{|r_i - r|^3} + \frac{r_i \cdot (Q_i \times r_i)}{|r_i - r|^5}$$

where q_i , p_i , Q_i are the charge, dipole moment and quadrupole moment respectively of the i -th atom of the ligand, while r_i is the position vector of the i -th atom. All the charges and moments are extracted from *ab initio* calculations (*vide supra*) followed by a LOPROP¹³ analysis of the electronic density. It is important to stress out that this method is an

analysis of the results of calculations done with high level of theory and therefore it does not have any prediction power by itself. The potential is calculated on a sphere with a radius given by the user and its intensity is represented with a color code (blue = low potential, red = high potential). For the sake of graphics, it can be represented as irregular surfaces in which the height of the surface is also proportional to the value of the potential. This representation is considered more intuitive. The code can also represent individually each component (charge, dipole and quadrupole potential) to give insights on which part is the dominant one.

Calculation of dipolar couplings: For the calculation of the isotropic dipolar coupling, we considered the anisotropy of each center as locally Ising ($g_{xx} = g_{yy} = 0$) and therefore we employed the following equation:

$$J_{ij}^{dipolar} = \frac{\mu_B^2}{3R^3} (g_{zzi} g_{zzj} (\cos\gamma_{ij} - 3\cos\theta_i \cos\theta_j))$$

Where μ_B^2 is the Bohr magneton, R is the distance between the centers (the module of the distance vector), g_{zz}^i is the component along the z-direction of the g-tensor for the i -th-center, θ_i is the angle between the distance vector and the eigenvector of the g-tensor corresponding to g_{zz}^i (the anisotropy axis) and γ_{ij} is the angle between the anisotropy axis of the two centers. It was not possible to include in our calculation any kind of exchange interaction (not even with a Lines model) between the nearest neighbors: the not-negligible dipolar interactions have an extension until ~12 Å and so, to model properly both dipolar and exchange interactions, it would have been necessary to include a total of 12 metallic ions. Clearly such calculation is too demanding in terms of hardware resources. Moreover the strength of the close range interactions (see J_1 and J_2 in Table S4) poses a not trivial issue in the fitting of a $J_{exchange}$ parameter, since we expect it orders of magnitude lower than the first-neighbor J_{dip} . Therefore, the variance of the exchange parameter, in the Lines model, would be too high to allow a quantitative analysis.

Additional information about *ab-initio* calculations are provided as supplementary information.

Acknowledgements

We acknowledge financial support from INSA Rennes, Rennes Metropole, China Scholarship Council, CNRS, Université de Rennes 1 and Region Bretagne. K. B. acknowledges Institut Universitaire de France, G. F. G. gratefully acknowledges the European Commission through the ERC-AdG 267746 MolNanoMas (project no. 267746) and the ANR (ANR-13-BS07-0022-01) for financial support. B. L. G. and G. F. G. thank the French GENCI/IDRIS-CINES centre for high-performance computing resources.

Keywords: lanthanides • metal-organic framework • single-chain magnet • single-molecule magnet • ferromagnetic coupling.

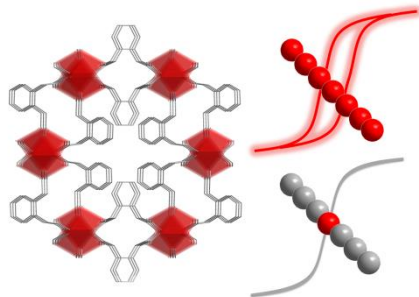
- [1] Liu, K.; Zhang, X.; Meng, X.; Shi, W.; Cheng, P.; Powell, A. K. *Chem. Soc. Rev.* **2016**, *45*, 2423-2439.
- [2] Liu, K.; Li, H.; Zhang, X.; Shi, W.; Cheng, P. *Inorg. Chem.* **2015**, *54*, 10224-10231.
- [3] Gao, S. *Molecular nanomagnets and related phenomena*; Springer, 2015; Vol. 164.
- [4] Benelli, C.; Gatteschi, D. *Introduction to Molecular Magnetism: From Transition Metals to Lanthanides*; Wiley, 2015.
- [5] Jeon, I. R.; Clérac, R. *Dalton Trans.* **2012**, *41*, 9569-9586.
- [6] Miyasaka, H.; Julve, M.; Yamashita, M.; Clerac, R. *Inorg. Chem.* **2009**, *48*, 3420-3437.

- [7] Coulon, C.; Miyasaka, H.; Clérac, R. In *Single-Molecule Magnets and Related Phenomena*; Winpenny, R., Ed.; Springer Berlin Heidelberg: 2006; Vol. 122, p 163-206.
- [8] Guillou, O.; Daiguebonne, C. In *Handbook on the Physics and Chemistry of Rare Earths [vol 34]*; Gschneider, K. A., Bünzli, J.-C. G., Pecharsky, V. K., Eds.; Elsevier 2005; Vol. 34, p 359-404.
- [9] Woodruff, D. N.; Winpenny, R. E. P.; Layfield, R. A. *Chem. Rev.* **2013**, *113*, 5110-5148.
- [10] Ungur, L.; Chibotaru, L. F. *Chem. Eur. J.* **2017**, *23*, 3708-3718.
- [11] Guo, F.-S.; Day, B. M.; Chen, Y.-C.; Tong, M.-L.; Mansikamäkki, Layfield, R. A. *Angew. Chem.-Int. Ed.* **2017**, *56*, 11445-11449.
- [12] Pugh, T.; Chilton, N. F.; Layfield, R. A. *Angew. Chem.-Int. Ed.* **2016**, *55*, 11082-11085.
- [13] Harriman, K. L. M.; Brosmer, J. L.; Ungur, L.; Diaconescu, P. L.; Murugesu, M. *J. Am. Chem. Soc.* **2017**, *139*, 1420-1423.
- [14] Ishikawa, N.; Sugita, M.; Ishikawa, T.; Koshihara, S.-y.; Kaizu, Y. *J. Am. Chem. Soc.* **2003**, *125*, 8694-8695.
- [15] Ishikawa, N. *Polyhedron* **2007**, *26*, 2147-2153.
- [16] Ganivet, C. R.; Ballesteros, B.; de la Torre, G.; Clemente-Juan, J. M.; Coronado, E.; Torres, T. *Chem. Eur. J.* **2013**, *19*, 1457-1465.
- [17] Wang, H.; Wang, B.-W.; Bian, Y.; Gao, S.; Jiang, J. *Coord. Chem. Rev.* **2016**, *306*, 195-216.
- [18] Jiang, S.-D.; Wang, B.-W.; Su, G.; Wang, Z.-M.; Gao, S. *Angew. Chem.-Int. Ed.* **2010**, *49*, 7448-7451.
- [19] Le Roy, J. J.; Korobkov, I.; Kim, J. E.; Schelter, E. J.; Murugesu, M. *Dalton Trans.* **2014**, *43*, 2737-2740.
- [20] Le Roy, J. J.; Gorelsky, S. I.; Korobkov, I.; Murugesu, M. *Organometallics* **2015**, *34*, 1415-1418.
- [21] Le Roy, J. J.; Jeletic, M.; Gorelsky, S. I.; Korobkov, I.; Ungur, L.; Chibotaru, L. F.; Murugesu, M. *J. Am. Chem. Soc.* **2013**, *135*, 3502-3510.
- [22] Ungur, L.; Le Roy, J. J.; Korobkov, I.; Murugesu, M.; Chibotaru, L. F. *Angew. Chem.-Int. Ed.* **2014**, *53*, 4413-4417.
- [23] Harriman, K. L. M.; Brosmer, J. L.; Ungur, L.; Diaconescu, P. L.; Murugesu, M. *J. Am. Chem. Soc.* **2017**, *139*, 1420-1423.
- [24] Meng, Y.-S.; Jiang, S.-D.; Wang, B.-W.; Gao, S. *Acc. Chem. Res.* **2016**, *49*, 2381-2389.
- [25] Lucaccini, E.; Briganti, M.; Perfetti, M.; Vendier, L.; Costes, J.-P.; Totti, F.; Sessoli, R.; Sorace, L. *Chem. Eur. J.* **2016**, *22*, 5552-5562.
- [26] Pointillart, F.; Cador, O.; Le Guennic, B.; Ouahab, L. *Coord. Chem. Rev.* **2017**, *346*, 150-175.
- [27] Layfield, R. A. *Organometallics* **2014**, *33*, 1084-1099.
- [28] Ding, Y.-S.; Chilton, N. F.; Winpenny, R. E. P.; Zheng, Y.-Z. *Angew. Chem.-Int. Ed.* **2016**, *55*, 16071-16074.
- [29] Goodwin, C. A. P.; Ortu, F.; Reta, D.; Chilton, N. F.; Mills, D. P. *Nature* **2017**, *548*, 439-442.
- [30] da Cunha, T. T.; Jung, J.; Boulon, M. E.; Campo, G.; Pointillart, F.; Pereira, C. L. M.; Le Guennic, B.; Cador, O.; Bernot, K.; Pineider, F.; Golhen, S.; Ouahab, L. *J. Am. Chem. Soc.* **2013**, *135*, 16332-16335.
- [31] Kou, H. Z.; Gao, S.; Li, C. H.; Liao, D. Z.; Zhou, B. C.; Wang, R. J.; Li, Y. D. *Inorg. Chem.* **2002**, *41*, 4756-4762.
- [32] Gao, C.; Yang, Q.; Wang, B.-W.; Wang, Z.-M.; Gao, S. *Crystengcomm* **2016**, *18*, 4165-4171.
- [33] Yi, X.; Bernot, K.; Pointillart, F.; Poneti, G.; Calvez, G.; Daiguebonne, C.; Guillou, O.; Sessoli, R. *Chem.-Eur. J.* **2012**, *18*, 11379-11387.
- [34] Cornia, A.; Mannini, M. In *Molecular Nanomagnets and Related Phenomena*; Springer Berlin Heidelberg: 2014, p 1-38.
- [35] Holmberg, R. J.; Murugesu, M. *J. Mater. Chem. C* **2015**, *3*, 11986-11998.
- [36] Mannini, M.; Pineider, F.; Sainctavit, P.; Danieli, C.; Otero, E.; Sciancalepore, C.; Talarico, A. M.; Arrio, M. A.; Cornia, A.; Gatteschi, D.; Sessoli, R. *Nat. Mater.* **2009**, *8*, 194-197.
- [37] Mannini, M.; Bertani, F.; Tudisco, C.; Malavolti, L.; Poggini, L.; Misztal, K.; Menozzi, D.; Motta, A.; Otero, E.; Ohresser, P.; Sainctavit, P.; Condorelli, G. G.; Dalcanale, E.; Sessoli, R. *Nat. Commun.* **2014**, *5*.
- [38] Margheriti, L.; Chiappe, D.; Mannini, M.; Car, P. E.; Sainctavit, P.; Arrio, M. A.; de Mongeot, F. B.; Cezar, J. C.; Piras, F. M.; Magnani, A.; Otero, E.; Caneschi, A.; Sessoli, R. *Adv. Mater.*, **22**, 5488-5493.
- [39] Malavolti, L.; Mannini, M.; Car, P.-E.; Campo, G.; Pineider, F.; Sessoli, R. *J. Mater. Chem. C* **2013**, *1*, 2935-2942.
- [40] Hofmann, A.; Salman, Z.; Mannini, M.; Amato, A.; Malavolti, L.; Morenzoni, E.; Prokscha, T.; Sessoli, R.; Suter, A. *ACS Nano* **2012**, *6*, 8390-8396.
- [41] Kiefl, E.; Mannini, M.; Bernot, K.; Yi, X.; Amato, A.; Leviant, T.; Magnani, A.; Prokscha, T.; Suter, A.; Sessoli, R.; Salman, Z. *ACS Nano* **2016**, *10*, 5663-5669.
- [42] Cimatti, I.; Yi, X.; Sessoli, R.; Puget, M.; Le Guennic, B.; Jung, J.; Guizouarn, T.; Magnani, A.; Bernot, K.; Mannini, M. *Appl. Surf. Sci.* **2017**, *in press*.
- [43] Yi, X.; Calvez, G.; Daiguebonne, C.; Guillou, O.; Bernot, K. *Inorg. Chem.* **2015**, *54*, 5213-5219.
- [44] Sessoli, R.; Bernot, K. In *Lanthanides and Actinides in Molecular Magnetism*; Wiley-VCH Verlag GmbH & Co. KGaA: 2015, p 89-124.
- [45] Liu, C.-M.; Zhang, D.; Hao, X.; Zhu, D.-B. *ACS Omega* **2016**, *1*, 286-292.
- [46] Liu, C.-M.; Zhang, D.-Q.; Zhao, Y.-S.; Hao, X.; Zhu, D.-B. *Inorg. Chem. Front.* **2016**, *3*, 1076-1081.
- [47] Liu, C.-M.; Zhang, D.-Q.; Zhu, D.-B. *Chem. Commun.* **2016**, *52*, 4804-4807.
- [48] Liu, C.-M.; Xiong, J.; Zhang, D.-Q.; Wang, B.-W.; Zhu, D.-B. *RSC Adv.* **2015**, *5*, 104854-104861.
- [49] Chen, M.; Sañudo, E. C.; Jiménez, E.; Fang, S.-M.; Liu, C.-S.; Du, M. *Inorg. Chem.* **2014**, *53*, 6708-6714.
- [50] Akhtar, M. N.; Chen, Y.-C.; AlDamen, M. A.; Tong, M.-L. *Dalton Trans.* **2017**, *46*, 116-124.
- [51] Campo, J.; Falvello, L. R.; Forcen-Vazquez, E.; Saenz de Pipaon, C.; Palacio, F.; Tomas, M. *Dalton Trans.* **2016**, *45*, 16764-16768.
- [52] Lin, P. H.; Burchell, T. J.; Clerac, R.; Murugesu, M. *Angew. Chem.-Int. Ed.* **2008**, *47*, 8848-8851.
- [53] Ren, Y.-X.; Zheng, X.-J.; Li, L.-C.; Yuan, D.-Q.; An, M.; Jin, L.-P. *Inorg. Chem.* **2014**, *53*, 12234-12236.
- [54] Liu, C.-M.; Zhang, D.-Q.; Hao, X.; Zhu, D.-B. *RSC Adv.* **2015**, *5*, 92980-92987.
- [55] Ma, X.; Xu, N.; Gao, C.; Li, L.; Wang, B.; Shi, W.; Cheng, P. *Dalton Trans.* **2015**, *44*, 5276-5279.
- [56] Chen, Z.; Zhao, B.; Cheng, P.; Zhao, X. Q.; Shi, W.; Song, Y. *Inorg. Chem.* **2009**, *48*, 3493-3495.
- [57] Yi, X. H.; Bernot, K.; Calvez, G.; Daiguebonne, C.; Guillou, O. *Eur. J. Inorg. Chem.* **2013**, 5879-5885.
- [58] Lunghi, A.; Totti, F.; Sessoli, R.; Sanvito, S. *Nat. Commun.* **2017**, *8*, 14620.
- [59] Coronado, E.; Minguez Espallargas, G. *Chem. Soc. Rev.* **2013**, *42*, 1525-1539.
- [60] Zhang, X.; Vieru, V.; Feng, X.; Liu, J.-L.; Zhang, Z.; Na, B.; Shi, W.; Wang, B.-W.; Powell, A. K.; Chibotaru, L. F.; Gao, S.; Cheng, P.; Long, J. R. *Angew. Chem.-Int. Ed.* **2015**, *54*, 9861-9865.
- [61] Sharples, J. W.; Collison, D. In *Lanthanides and Actinides in Molecular Magnetism*; Wiley-VCH Verlag GmbH & Co. KGaA: 2015, p 293-314.
- [62] Lorusso, G.; Sharples, J. W.; Palacios, E.; Roubeau, O.; Brechin, E. K.; Sessoli, R.; Rossin, A.; Tuna, F.; McInnes, E. J. L.; Collison, D.; Evangelisti, M. *Adv. Mater.* **2013**, *25*, 4653-4656.
- [63] Sibille, R.; Mazet, T.; Malaman, B.; François, M. *Chem. Eur. J.* **2012**, *18*, 12970-12973.
- [64] Lorusso, G.; Palacios, M. A.; Nichol, G. S.; Brechin, E. K.; Roubeau, O.; Evangelisti, M. *Chem. Commun.* **2012**, *48*, 7592-7594.
- [65] Tian, H.; Wang, X.; Mei, X.; Liu, R.; Zhu, M.; Zhang, C.; Ma, Y.; Li, L.; Liao, D. *Eur. J. Inorg. Chem.* **2013**, 1320-1325.
- [66] Bartolome, E.; Bartolome, J.; Melnic, S.; Prodius, D.; Shova, S.; Arauzo, A.; Luzon, J.; Badia-Romano, L.; Luis, F.; Turta, C. *Dalton Trans.* **2014**, *43*, 10999-11013.

- [67] Bartolome, E.; Bartolome, J.; Melnic, S.; Prodius, D.; Shova, S.; Arauzo, A.; Luzon, J.; Luis, F.; Turta, C. *Dalton Trans.* **2013**, *42*, 10153-10171.
- [68] Liu, R. N.; Zhang, C. M.; Mei, X. L.; Hu, P.; Tian, H. X.; Li, L. C.; Liao, D. Z.; Sutter, J. P. *New J. Chem.* **2012**, *36*, 2088-2093.
- [69] Guo, Y.; Xu, G. F.; Wang, C.; Cao, T. T.; Tang, J. K.; Liu, Z. Q.; Ma, Y.; Yan, S. P.; Cheng, P.; Liao, D. Z. *Dalton Trans.* **2012**, *41*, 1624-1629.
- [70] Evangelisti, M.; Luis, F.; Mettes, F. L.; Aliaga, N.; Aromí, G.; Alonso, J. J.; Christou, G.; de Jongh, L. J. *Phys. Rev. Lett.* **2004**, *93*, 117202.
- [71] Benelli, C.; Caneschi, A.; Gatteschi, D.; Sessoli, R. *Adv. Mater.* **1992**, *4*, 504-505.
- [72] Chen, L.-J.; Chen, X.; Hou, Q.-B.; Yang, M.-X.; Lin, S. *Chinese J. Inorg. Chem.* **2014**, *30*, 786-792.
- [73] Wang, C.-Y.; Wu, X.-S.; Li, X. *Chinese J. Inorg. Chem.* **2008**, *24*, 781-784.
- [74] Zhang, M.-L.; Chen, X.-L.; Wang, J.-J. *Chinese J. Struct. Chem.* **2014**, *33*, 935-941.
- [75] Li, X.; Wang, C.; Zheng, X.; Zou, Y. *J. Coord. Chem.* **2008**, *61*, 1127-1136.
- [76] Yi, X.; Bernot, K.; Pointillart, F.; Poneti, G.; Calvez, G.; Daigebonne, C.; Guillou, O.; Sessoli, R. *Chem. Eur. J.* **2012**, *18*, 11379-11387.
- [77] Lin, P.-H.; Burchell, T. J.; Clérac, R.; Murugesu, M. *Angew. Chem.-Int. Ed.* **2008**, *120*, 8980-8983.
- [78] Biswas, S.; Das, S.; Rogez, G.; Chandrasekhar, V. *Eur. J. Inorg. Chem.* **2016**, 3322-3329.
- [79] Alvarez, S.; Alemany, P.; Casanova, D.; Cirera, J.; Llunell, M.; Avnir, D. *Coord. Chem. Rev.* **2005**, *249*, 1693-1708.
- [80] Bartolome, E.; Bartolome, J.; Arauzo, A.; Luzon, J.; Badia, L.; Cases, R.; Luis, F.; Melnic, S.; Prodius, D.; Shova, S.; Turta, C. *J. Mater. Chem. C* **2016**, *4*, 5038-5050.
- [81] Jung, J.; Le Natur, F.; Cador, O.; Pointillart, F.; Calvez, G.; Daigebonne, C.; Guillou, O.; Guizouarn, T.; Le Guennic, B.; Bernot, K. *Chem. Commun.* **2014**, *50*, 13346-13348.
- [82] Gómez-Coca, S.; Aravena, D.; Morales, R.; Ruiz, E. *Coord. Chem. Rev.* **2015**, *289-290*, 379-392.
- [83] Luo, Y.-d.; Sun, G.-m.; Li, D.-m.; Luo, F. *Inorg. Chem. Commun.* **2011**, *14*, 778-780.
- [84] Su, L.; Song, W.-C.; Zhao, J.-P.; Liu, F.-C. *Chem. Commun.* **2016**, *52*, 8722-8725.
- [85] Arosio, P. C., M.; Mariani, M.; Orsini, F.; Bogani, L.; Caneschi, A.; Lago, J.; Lascialfari, A. *J. Appl. Phys.* **2015**, *117*, 17B310.
- [86] Hui, Y.-C.; Meng, Y.-S.; Li, Z.; Chen, Q.; Sun, H.-L.; Zhang, Y.-Q.; Gao, S. *Crystengcomm* **2015**, *17*, 5620-5624.
- [87] Vaz, M. G. F.; Cassaro, R. A. A.; Akpinar, H.; Schlueter, J. A.; Lahti, P. M.; Novak, M. A. *Chem. Eur. J.* **2014**, *20*, 5460-5467.
- [88] Bernot, K.; Bogani, L.; Sessoli, R.; Gatteschi, D. *Inorg. Chim. Acta* **2007**, *360*, 3807-3812.
- [89] Bogani, L.; Sangregorio, C.; Sessoli, R.; Gatteschi, D. *Angew. Chem.-Int. Ed.* **2005**, *117*, 5967-5971.
- [90] Coulon, C.; Miyasaka, H.; Clerac, R. In *Single-Molecule Magnets and Related Phenomena*; Winpenny, R., Ed.; Springer-Verlag Berlin: Berlin, 2006; Vol. 122, p 163-206.
- [91] Saitoh, A.; Miyasaka, H.; Yamashita, M.; Clerac, R. *J. Mater. Chem.* **2007**, *17*, 2002-2012.
- [92] Billoni, O. V. P., V.; Pescia, D.; Vindigni, A. *Phys. Rev. B* **2011**, *84*.
- [93] Zheng, Y.-Z.; Lan, Y.; Wernsdorfer, W.; Anson, C. E.; Powell, A. K. *Chem. Eur. J.* **2009**, *15*, 12566-12570.
- [94] Bernot, K.; Bogani, L.; Caneschi, A.; Gatteschi, D.; Sessoli, R. *J. Am. Chem. Soc.* **2006**, *128*, 7947-7956.
- [95] Bogani, L.; Vindigni, A.; Sessoli, R.; Gatteschi, D. *J. Mater. Chem.* **2008**, *18*, 4750-4758.
- [96] Hu, P.; Wang, X.; Ma, Y.; Wang, Q.; Li, L.; Liao, D. *Dalton Trans.* **2014**, *43*, 2234-2243.
- [97] Gatteschi, D. S., R.; Caneschi, A.; Bogani, L.; Vindigni, A. In *225th National Meeting of the American-Chemical-Society: New Orleans, Louisiana, 2003*; pp U147-U147.
- [98] Chibotaru, L. F.; Ungur, L.; Soncini, A. *Angew. Chem.-Int. Edit.* **2008**, *47*, 4126-4129.
- [99] Liddle, S. T.; van Slageren, J. *Chem. Soc. Rev.* **2015**, *44*, 6655-6669.
- [100] Selvanathan, P.; Huang, G.; Guizouarn, T.; Roisnel, T.; Fernandez-Garcia, G.; Totti, F.; Le Guennic, B.; Calvez, G.; Bernot, K.; Norel, L.; Rigaut, S. *Chem. Eur. J.* **2016**, *22*, 15222-15226.
- [101] Pointillart, F.; Bernot, K.; Golhen, S.; Le Guennic, B.; Guizouarn, T.; Ouahab, L.; Cador, O. *Angew. Chem.-Int. Ed.* **2015**, *54*, 1504-1507.
- [102] Zhang, D.; Tian, Y.-M.; Sun, W.-B.; Li, H.-F.; Chen, P.; Zhang, Y.-Q.; Yan, P.-F. *Dalton Trans.* **2016**, *45*, 2674-2680.
- [103] Meng, Y.-S.; Qiao, Y.-S.; Zhang, Y.-Q.; Jiang, S.-D.; Meng, Z.-S.; Wang, B.-W.; Wang, Z.-M.; Gao, S. *Chem. Eur. J.* **2016**, *22*, 4704-4708.
- [104] Calahorra, A. J.; Oyarzabal, I.; Fernandez, B.; Seco, J. M.; Tian, T.; Fairen-Jimenez, D.; Colacio, E.; Rodriguez-Dieguez, A. *Dalton Trans.* **2016**, *45*, 591-598.
- [105] Amjad, A.; Madalan, A. M.; Andruh, M.; Caneschi, A.; Sorace, L. *Chem. Eur. J.* **2016**, *22*, 12849-12858.
- [106] Biltmo, A. H., P. *Phys. Rev. B* **2008**, *78*.
- [107] Gannarelli, C. M. S. S., D. M.; Rosenbaum, T. F.; Aepli, G.; Fisher, A. *J. Phys. Rev. B* **2012**, *86*.
- [108] Habib, F.; Lin, P.-H.; Long, J.; Korobkov, I.; Wernsdorfer, W.; Murugesu, M. *J. Am. Chem. Soc.* **2011**, *133*, 8830-8833.
- [109] Liu, J.; Chen, Y.-C.; Lai, J.-J.; Wu, Z.-H.; Wang, L.-F.; Li, Q.-W.; Huang, G.-Z.; Jia, J.-H.; Tong, M.-L. *Inorg. Chem.* **2016**, *55*, 3145-3150.
- [110] Popova, M. N. C., E. P.; Malkin, B. Z.; Saikin, S. K. *Phys. Rev. B* **2000**, *61*, 7421-7427.
- [111] Quilliam, J. A. M., S.; Kycia, J. B. *Phys. Rev. B* **2012**, *85*.
- [112] Rodriguez, J. A., A. A.; Carlo, J. P.; Dunsiger, S. R.; MacDougall, G. J.; Russo, P. L.; Savici, A. T.; Uemura, Y. J.; Wiebe, C. R.; Luke, G. M. *Phys. Rev. Lett.* **2010**, *105*.
- [113] Schlegel, C.; Burzurí, E.; Luis, F.; Moro, F.; Manoli, M.; Brechin, E. K.; Murrie, M.; van Slageren, J. *Chem. Eur. J.* **2010**, *16*, 10178-10185.
- [114] van Slageren, J.; Dengler, S.; Gomez-Segura, J.; Ruiz-Molina, D.; Dressel, M. *Inorg. Chim. Acta* **2008**, *361*, 3714-3717.
- [115] Vergnani, L.; Barra, A.-L.; Neugebauer, P.; Rodriguez-Douton, M. J.; Sessoli, R.; Sorace, L.; Wernsdorfer, W.; Cornia, A. *Chem. Eur. J.* **2012**, *18*, 3390-3398.
- [116] Moro, F.; Kaminski, D.; Tuna, F.; Whitehead, G. F. S.; Timco, G. A.; Collison, D.; Winpenny, R. E. P.; Ardavan, A.; McInnes, E. J. L. *Chem. Commun.* **2014**, *50*, 91-93.
- [117] Meihaus, K. R.; Rinehart, J. D.; Long, J. R. *Inorg. Chem.* **2011**, *50*, 8484-8489.
- [118] Ishii, N.; Okamura, Y.; Chiba, S.; Nogami, T.; Ishida, T. *J. Am. Chem. Soc.* **2008**, *130*, 24-25.
- [119] Coulon, C.; Clérac, R.; Wernsdorfer, W.; Colin, T.; Miyasaka, H. *Phys. Rev. Lett.* **2009**, *102*, 167204.
- [120] Gavrilenko, K. S.; Cador, O.; Bernot, K.; Rosa, P.; Sessoli, R.; Golhen, S.; Pavlishchuk, V. V.; Ouahab, L. *Chem.-Eur. J.* **2008**, *14*, 2034-2043.
- [121] Miyasaka, H.; Takayama, K.; Saitoh, A.; Furukawa, S.; Yamashita, M.; Clérac, R. *Chem. Eur. J.* **2010**, *16*, 3656-3662.
- [122] Bhowmick, I.; Hillard, E. A.; Dechambenoit, P.; Coulon, C.; Harris, T. D.; Clerac, R. *Chem. Commun.* **2012**, *48*, 9717-9719.
- [123] Prins, F.; Pasca, E.; de Jongh, L. J.; Kooijman, H.; Spek, A. L.; Tanase, S. *Angew. Chem.-Int. Edit.* **2007**, *46*, 6081-6084.
- [124] Palacios, M. A.; Titos-Padilla, S.; Ruiz, J.; Herrera, J. M.; Pope, S. J. A.; Brechin, E. K.; Colacio, E. *Inorg. Chem.* **2014**, *53*, 1465-1474.
- [125] Pointillart, F.; Kuropatov, V.; Mitin, A.; Maury, O.; Le Gal, Y.; Golhen, S.; Cador, O.; Cherkasov, V.; Ouahab, L. *Eur. J. Inorg. Chem.* **2012**, *2012*, 4708-4718.
- [126] Wernsdorfer, W.; Aliaga-Alcalde, N.; Hendrickson, D. N.; Christou, G. *Nature* **2002**, *416*, 406-409.
- [127] Nguyen, T. N.; Wernsdorfer, W.; Shiddiq, M.; Abboud, K. A.; Hill, S.; Christou, G. *Chem. Sci.* **2016**, *7*, 1156-1173.
- [128] Nava, A.; Rigamonti, L.; Zangrando, E.; Sessoli, R.; Wernsdorfer, W.; Cornia, A. *Angew. Chem.-Int. Ed.* **2015**, *54*, 8777-8782.

- [129] Pinkowicz, D.; Southerland, H. I.; Avendaño, C.; Prosvirin, A.; Sanders, C.; Wernsdorfer, W.; Pedersen, K. S.; Dreiser, J.; Clérac, R.; Nehrkorn, J.; Simeoni, G. G.; Schnegg, A.; Holldack, K.; Dunbar, K. R. *J. Am. Chem. Soc.* **2015**, *137*, 14406-14422.
- [130] Poneti, G.; Bernot, K.; Bogani, L.; Caneschi, A.; Sessoli, R.; Wernsdorfer, W.; Gatteschi, D. *Chem. Commun.* **2007**, 1807-1809.
- [131] Yi, X.; Bernot, K.; Cador, O.; Luzon, J.; Calvez, G.; Daiguebonne, C.; Guillou, O. *Dalton Trans.* **2013**, *42*, 6728-6731.
- [132] Fortea-Perez, F. R.; Mon, M.; Ferrando-Soria, J.; Boronat, M.; Leyva-Perez, A.; Corma, A.; Herrera, J. M.; Osadchii, D.; Gascon, J.; Armentano, D.; Pardo, E. *Nat Mater* **2017**, *16*, 760-766.
- [133] Mon, M.; Ferrando-Soria, J.; Verdaguer, M.; Train, C.; Paillard, C.; Dkhil, B.; Versace, C.; Bruno, R.; Armentano, D.; Pardo, E. *J. Am. Chem. Soc.* **2017**, *139*, 8098-8101.
- [134] Vallejo, J.; Fortea-Perez, F. R.; Pardo, E.; Benmansour, S.; Castro, I.; Krzystek, J.; Armentano, D.; Cano, J. *Chem. Sci.* **2016**, *7*, 2286-2293.
- [135] Chen, Q.; Li, J.; Meng, Y.-S.; Sun, H.-L.; Zhang, Y.-Q.; Sun, J.-L.; Gao, S. *Inorg. Chem.* **2016**, *55*, 7980-7987.
- [136] Mastropietro, T. F.; Marino, N.; Munno, G. D.; Lloret, F.; Julve, M.; Pardo, E.; Armentano, D. *Inorg. Chem.* **2016**, *55*, 11160-11169.
- [137] Mon, M.; Pascual-Álvarez, A.; Grancha, T.; Cano, J.; Ferrando-Soria, J.; Lloret, F.; Gascon, J.; Pasán, J.; Armentano, D.; Pardo, E. *Chem. Eur. J.* **2016**, *22*, 539-545.
- [138] Aulakh, D.; Xie, H.; Shen, Z.; Harley, A.; Zhang, X.; Yakovenko, A. A.; Dunbar, K. R.; Wriedt, M. *Inorg. Chem.* **2017**, *56*, 6965-6972.
- [139] Li, Y.; Wang, T.; Meng, H.; Zhao, C.; Nie, M.; Jiang, L.; Wang, C. *Dalton Trans.* **2016**, *45*, 19226-19229.
- [140] Baldoví, J. J.; Coronado, E.; Gaita-Ariño, A.; Gamer, C.; Giménez-Marqués, M.; Mínguez Espallargas, G. *Chem. Eur. J.* **2014**, *20*, 10695-10702.

Ferromagnetic interactions induced by MOF architecture turn a poor SMM into a slow relaxing material



Gang Huang,^a Guglielmo Fernandez-Garcia,^{b,c} Insa Badiane,^{a,d} Magatte Camarra,^{a,d} Stéphane Freslon,^a Olivier Guillou,^a Carole Daiguebonne,^a Federico Totti,^c Olivier Cador,^b Thierry Guizouarn,^b Boris Le Guennic^{a,b} and Kevin Bernot*

Magnetic slow relaxation in a Metal Organic Framework made of chains of ferromagnetically coupled Single-Molecule Magnets